

Antimicrobial, antioxidant and cytotoxic effect of Molybdenum trioxide nanoparticles and application of this for degradation of ketamine under different light illumination



Ali Fakhri ^{a,*}, Pedram Afshar Nejad ^b

^a Young Researchers and Elites Club, Science and Research Branch, Islamic Azad University, Tehran, Iran

^b Department of Microbiology, Ayatollah Amoli Branch, Islamic Azad University, Amol, Iran

ARTICLE INFO

Article history:

Received 1 October 2015

Received in revised form 1 April 2016

Accepted 4 April 2016

Available online 08 April 2016

Keywords:

MoO₃ NPs

Drug

Degradation

Antibacterial

Antioxidant

Cytotoxicity

ABSTRACT

A hydrothermal method was employed to synthesize Molybdenum trioxide (MoO₃) nanoparticles. The synthesized samples were evaluated for photocatalytic properties and biological application. The nanoparticles characterized by scanning electron microscopy, powder X-ray diffraction, transmission electron microscopy, an energy dispersive X-ray spectrometer and UV–Vis DRS spectra. The synthesized MoO₃ NPs were found to be spherical in shape with size in the range of 75 nm. The synthesized MoO₃ nanoparticles have good optical properties with 2.78 eV of band-gap. The photocatalytic properties of the synthesized MoO₃ nanoparticles were carried out by performing the degradation of ketamine under visible, UV and sunlight irradiations. A high efficiency was observed between sunlight and MoO₃ nanoparticles for the photocatalysis reaction. Two compounds as intermediates of photo-degradation of ketamine under visible and UV lights were detected. The antifungal activity of the nanoscale MoO₃ against *Candida albicans* and *Aspergillus niger* was assessed using the disc-diffusion susceptibility tests. All MoO₃ nanoparticles concentrations showed good ABT radical scavenging activity. Then, this research has been presented to exhibit the synthesized MoO₃ NPs which indicated a high antibacterial activity against Gram negative and positive bacteria and were also proved to exhibit excellent cytotoxic influence on lung and breast cancer cell lines. The results show that the high applicability of MoO₃ nanoparticles biologically was great and is environmentally friendly.

© 2016 Elsevier B.V. All rights reserved.

1. Introduction

The presence of pharmaceutical ingredients in aqueous environment has raised increasing concerns in recent years. Typical sources of them are animal excrements, hospital waste, and sewage effluents. These compound concentrations are much lower compared with other conventional organic pollutants, a wide range of investigations reported that these drugs have raised concerns due to their potential impact on human and environment [1,2].

From 2008, many developed countries began examining controlled drugs in surface waters and wastewater urban. The methamphetamine and ketamine were found in wastewater treatment plants at 296 and 147 ng/L [3].

Ketamine is a synthetic compound used as an anesthetic and analgesic drug and also (illicitly) as a hallucinogen. This is a noncompetitive N-methyl-D-aspartate (NMDA) receptor antagonist introduced recently for analgesia in patients with chronic pain. The role of the NMDA

receptor in processing nociceptive input and its ability to improve pain management and reduce opioid-related adverse effects have led to renewed clinical interest in ketamine [3].

Photocatalytic degradation of drug pollutants can be an effective alternative to biological methods for removal of drug contaminants. At present, UV disinfection is widely deployed in wastewater urban. Among many materials, semiconductors have shown as promise a photocatalyst because of its high chemical stability and photocatalytic reactivity [4–11].

MoO₃ is a large band gap semiconductor (2.90 eV) and, when crystallized, forms hexagonal or rectangular plates, depending on synthesis conditions [12]. Thermodynamically, the stability of the amorphous phases was lower than of orthorhombic MoO₃ [13]. This oxide is normally found in the orthorhombic phase, which is the main aim of much research due to its many applications [14–18]. This phase can be described as a layered structure formed by covalent double layers of MoO₆ octahedral [13,19–21].

The present study investigated to develop a photocatalytic active particle under different light; hence natural resource could be made use for the degradation pollutant bearing effluents.

* Corresponding author.

E-mail address: ali.fakhri88@yahoo.com (A. Fakhri).

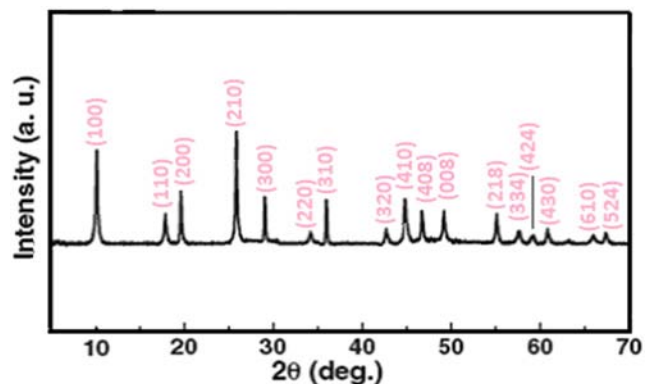


Fig. 1. X-ray diffraction analysis of MoO₃ NPs.

2. Materials and Methods

2.1. Materials

All the chemicals were obtained from Sigma-Aldrich Ltd., USA. All the chemicals used for the study were of analytical grade.

2.2. Preparation of MoO₃ NPs

The powders of 10 mL 0.2 M of ammonium heptamolybdate tetrahydrate were weighed into a Teflon-lined stainless steel autoclave of 50 mL capacity, and then 5 mL of 1.5 M HNO₃ aqueous solution was added in with stirring (the stirring was kept for a while until a

homogeneous solution was formed). The autoclaves containing the reaction solutions were sealed and maintained at 150 °C for 12 h, then cooled naturally to room temperature. The as-formed precipitates were filtered, washed with distilled water and ethanol, and finally dried in a vacuum at 100 °C for 3 h.

2.3. Characterization Instruments

An X-ray diffractometer (XRD) Philips X'Pert, transmission electron microscopy (TEM, JEM-2100F HR, 200 kV), a scanning electron microscope (SEM), and a JEOL JSM-5600 Digital Scanning Electron Microscope were used to characterize the nanopowders. UV–Vis DRS mensuration was performed in a double beam spectrophotometer (JASCO V-550). The catalyst compositions were analyzed with an energy dispersive X-ray spectrometer (EDX-700HS, SHIMADZU).

2.4. Evaluation of Photocatalytic Property

In the present research, degradation of ketamine as a pollutant by MoO₃ NPs was investigated using visible, UV and sunlight photocatalysis. The photocatalytic degradation was tested by photocatalysts and an aqueous solution of ketamine in an open cylindrical stainless glass vessel with a volume of 200 mL. In each experiment, 20 mg photocatalyst was suspended in 30 mL model ketamine aqueous solution with a concentration of 10 mg/L. Then, the suspended solution was placed in the dark for 30 min under magnetic stirring to check the adsorption–desorption capability. The concentration of ketamine after reaction was recorded as C_t and then experiments were carried out further for 60 min under visible (1000 W halogen) and UV lights (125 W UV lamp at 365 nm) light illumination. A second photoreactor for the solar photocatalysis experiments was constructed using a borosilicate

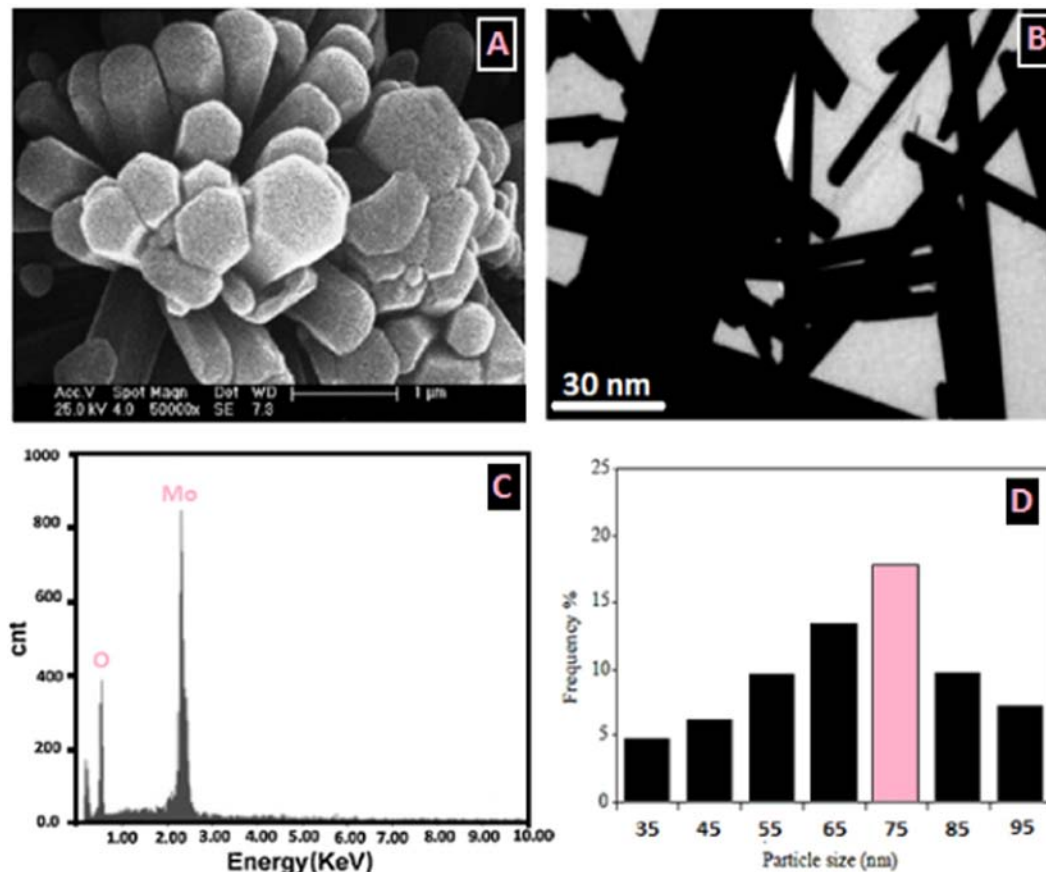


Fig. 2. SEM image (A), TEM image (B), EDX pattern (C), particle size distribution (D) of MoO₃ NPs.

glass container of 200 mL capacity, 100 mm internal diameter and 200 mm in height where sunlight was directed axially at the center of the reactor. The ketamine concentration was distinguished with the aid of a two dimensional Gas Chromatography (GC * GC) (Kimia Shangarf Pars Research Co., Iran).

2.5. HPLC Condition for Analysis of Intermediates of Photocatalysis Reaction

HPLC analysis was carried out on a Surveyor MS pump (Thermal Quest, U.S.A.). Chromatographic separation was performed on a Supelcosil™ LC-18 dB column (5 μm particle size) 4.6 × 250 mm with precolumn filter of 3 mm frit. The mobile phase consisted of acetonitrile: 0.03 M ammonium acetate buffer (50:50 by vol) adjusted to pH 7.1. The flow rate of the mobile phase was 1.0 mL/min.

2.6. The Antimicrobial Property

Pure bacterial cultures *Escherichia coli* (MTCC 443) and *Bacillus subtilis* (MTCC 441), were obtained from MTCC. A hole (6 mm) was bored aseptically in Muller Hinton agar medium with a sterile cork borer that was already seeded with test organisms. The holes were filled with different concentrations of MoO₃ NPs (10 μL) and stand for 1 h for the nanoparticles perfusion. The plates were stand for further incubation at 37 °C for 24 h. The antibacterial activity was measured in terms of the diameter (in millimeters) of the inhibition zone and compared with control. The experiment was performed in triplicates.

The antifungal activity of the all samples was evaluated against *Candida albicans* and *Aspergillus niger* using the disc-diffusion susceptibility method. 50 mL PDB medium was prepared by dissolving amount of potato dextrose powder (39 g/L) in Millipore water and mixed it properly. The final volume of 50 mL was made by adding adequate amount of Millipore water to it. Medium was then sterilized at 121 °C for 15 min. This medium was poured into five different sterilized petri dishes. After solidification of these media, 50 μL suspension cultures of *C. albicans* and *A. niger* were evenly dispersed on the solidified culture media surface. Then sterilized filter paper discs (6 mm diameter) were placed at the center of each petri dish. The all samples (concentrations = 10 mg/mL) were mixed with sterilized Millipore water using a low power sonicator. In the fifth petri dish the growth of *C. albicans* and *A. niger* was observed for the disc impregnated with only sterile Millipore water in the absence of samples and it was taken as the fungal control. Then the dishes were incubated in a thermostatic chamber at 28 °C for 72 h. All petri dishes were kept in regular observation to examine the

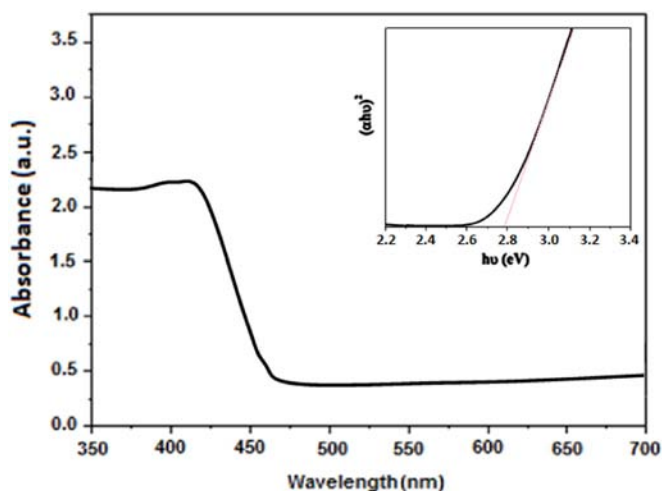


Fig. 3. UV-Vis absorption spectra and band gap energy estimation of MoO₃ nanoparticles (The inset is Kubelka–Munk plot).

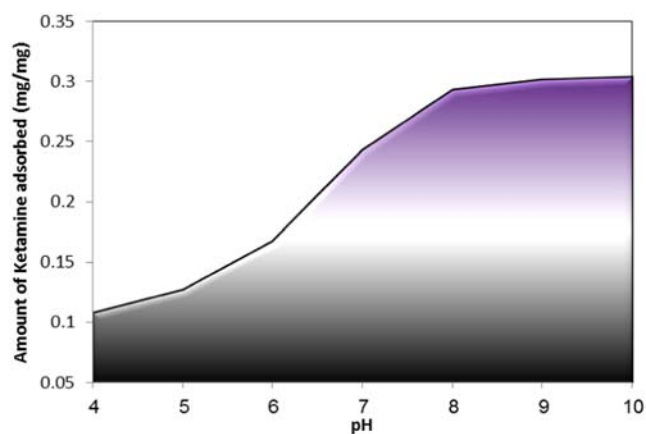


Fig. 4. Effect of pH on the adsorption of morphine on the surface of MoO₃ NPs in dark condition.

zone of inhibition around each disc. The diameters of the clear zone of inhibition were measured in millimeters (mm). To minimize experimental error the experiment was repeated several times.

2.7. Estimating Antioxidant Activity

ABTS radical cations were produced by reacting 7 mM of ABTS and 2.45 mM of potassium per sulphate solutions on incubating the mixture in dark place for 16 h at 25 °C. The solution was diluted with PBS to give an absorbance of 1.000. Different concentrations of the MoO₃ NPs in 10 μL were added to 140 μL of ABTS working solution and 50 μL of water to give a final volume of 200 μL. The absorbance was recorded immediately at 734 nm. BHT was used as reference standard. The amount inhibition was distinguished from the following equation:

$$\text{Inhibition(\%)} = \frac{\text{Absorbance of control} - \text{Absorbance of test sample}}{\text{Absorbance control}} \quad (1)$$

2.8. Cytotoxicity Assay

The cytotoxic influence of synthesized MoO₃ NPs was investigated by MTT assay using MCF-7 and HEP G2 cell lines. The cells were seeded

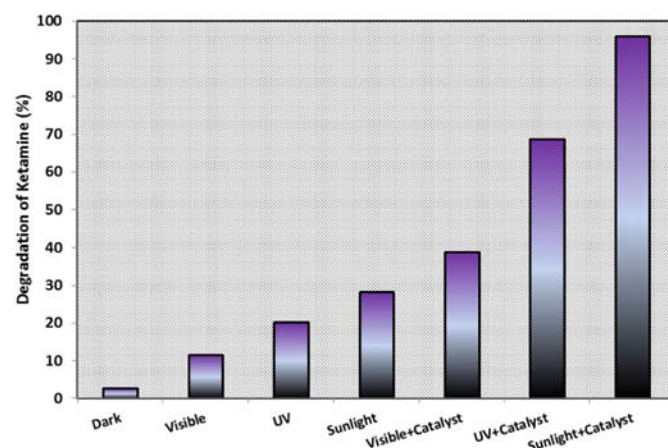


Fig. 5. Variation in the degradation of ketamine with or without catalyst under different modes of operations (pH = 8; concentration = 10 ppm; time = 30 min).

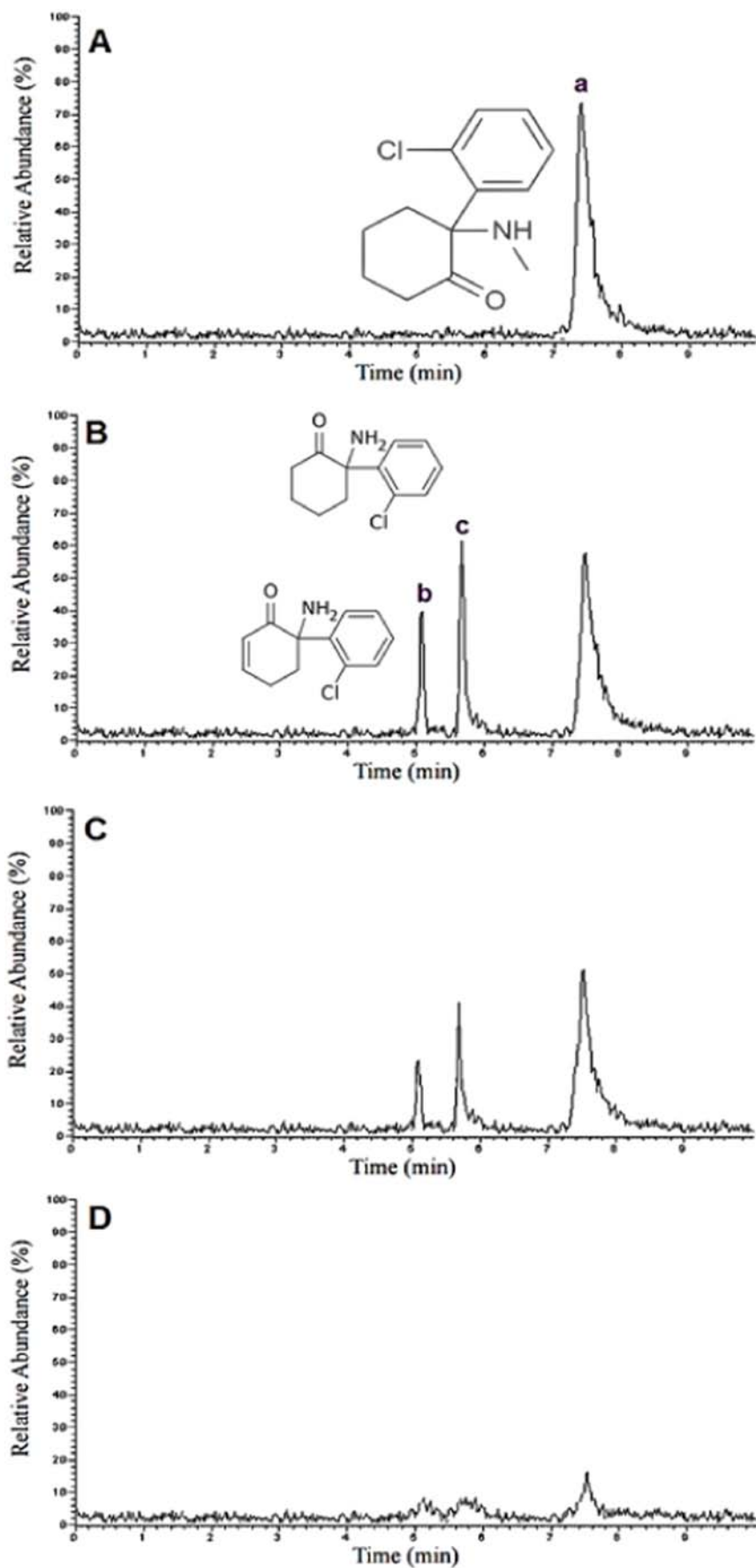


Fig. 6. High-performance liquid chromatograms of ketamine solution during photochemical degradation by MoO_3 NPs; (A) any without reaction, (B) under visible light, (C) under UV light, and (D) under sunlight irradiation.

in 24 well tissue culture plates at a density of 1×10^6 , allowed to attach for one day and treated with different concentrations (25–0.625 $\mu\text{g}/\text{mL}$) of MoO_3 NPs. After the MoO_3 NPs treatment, the medium was changed

and the cells were washed twice with MEM without FCS to remove the dead cells, the cells were incubated with 200 μL (5 mg/mL) of MTT for 6–7 h in 5% CO_2 incubator for cytotoxicity. Color development was measured by a spectrophotometer at 595 nm after cell lyses in DMSO. The viability was determined by using the following formula.

$$\text{Cell viability}(\%) = \frac{\text{Mean OD} \times 100}{\text{Control OD}} \quad (2)$$

3. Results and Discussion

3.1. Characterization of the MoO_3 NPs

The X-ray diffraction pattern shown in Fig. 1 describes the phase composition and crystal structure of MoO_3 nanomaterials. The strong peaks at (100) & (210) show crystalline nature of nanomaterials. It can be seen in orthorhombic lattice system with lattice parameter of $a = 11.92 \text{ \AA}$ and $c = 16.01 \text{ \AA}$ (JCPDS: 21–0569). No obvious diffraction patterns were found that show the phase purity of the synthesized products. The crystallite size can be estimated from the full width half maximum (FWHM) values found from the predominant (021) diffraction peak at 25.7° according to the following Debye–Scherrer equation, $D = 0.9\lambda / \beta \cos\theta$ [21,22], where λ is the wavelength of Cu radiation (1.5406 Å), and β is the Bragg diffraction angle. The calculated crystallite size was around 75 nm.

Fig. 2A and 2B shows SEM and TEM images of synthesized MoO_3 . The synthesized material is shaped like clusters of hexagonal rods. Result from the EDX spectra indicates that the nanorods contain only oxygen and molybdenum elements (Fig. 2(C)). Fig. 2(D) indicates the particle size plot for MoO_3 nanoparticles. The mean size distribution of MoO_3 NPs is 75 nm.

Fig. 3A shows UV–Vis absorption spectra of MoO_3 NPs. Optical absorption spectra indicate weak absorption peak at around 430 nm. The MoO_3 NPs has good absorption for light in this wavelength. The absorption edge shifted towards the shorter wavelength side. The direct band gap energy can be determined from a plot of $(\alpha h\nu)^2$ vs. photon energy ($h\nu$). The value of energy band gap was distinguished by using the equations

$$\alpha h\nu = A(h\nu - E_g)^n \quad (3)$$

$$(\alpha h\nu)^2 = A(h\nu - E_g) \quad (4)$$

where α = absorption coefficient, $h\nu$ = photon energy, A = constant, E_g = energy band gap, $n = 1/2$ for the allowed direct band gap. The exponent n depends on the type of transition (values 1/2, 2, 3/2 and 3) and corresponds to the allowed direct, allowed indirect, forbidden direct and forbidden indirect transitions [23]. The value of direct band gap was determined by $(\alpha h\nu)^2$ vs. $h\nu$ graph (the inset of Fig. 3). The band-gap of MoO_3 NPs was computed as 2.78 eV.

Table 1

Zone of inhibition (mm) of MoO_3 NPs against antibacterial and antifungal pathogens.

Organism	MoO_3 nanoparticles	Control
Antibacterial activity		
<i>Escherichia coli</i>	13.41 \pm 0.41	4.21 \pm 0.25
<i>Bacillus subtilis</i>	11.27 \pm 0.37	3.15 \pm 0.53
Antifungal activity		
<i>Candida albicans</i>	21.54 \pm 0.28	6.72 \pm 0.82
<i>Aspergillus niger</i>	19.95 \pm 0.58	6.56 \pm 0.41

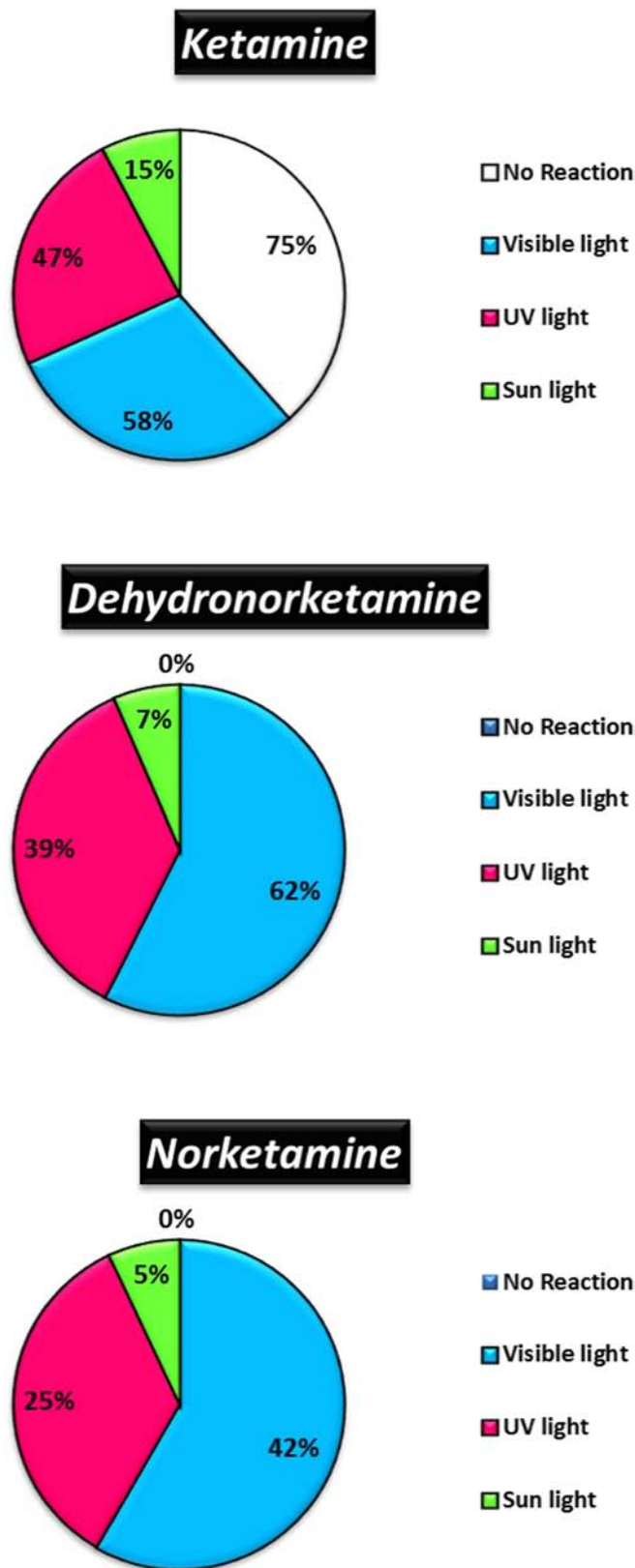


Fig. 7. The percentage of degraded product in any condition of reaction.

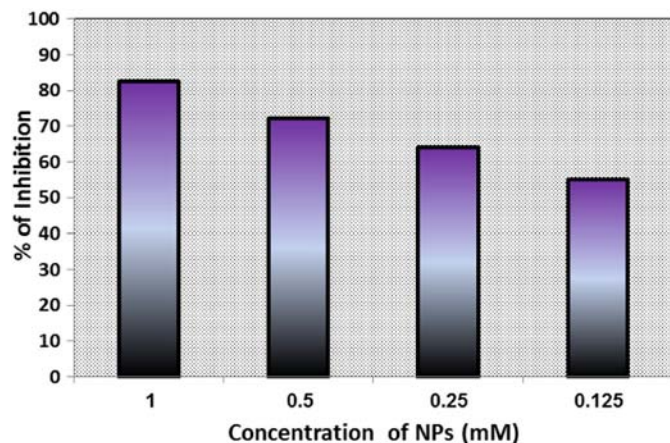


Fig. 8. Percentage of inhibition MoO₃ NPs for antioxidant activity.

3.2. Adsorption Process

The adsorption characteristics of ketamine on the surface of NPs are very important in photo-degradation reaction. The adsorption process may be influenced by pH of the interaction medium due to the modification of the electrical double layer of the solid electrolyte interface [24]. Therefore, the present study used different pH in order to investigate the pH effect on adsorption of ketamine on MoO₃ NPs in dark condition (Fig. 4). The pH of samples was adjusted by using 0.1 N NaOH or HCl solutions. The adsorption reactions were completed in 30 min interaction.

3.3. Degradation Process

For evaluating of photocatalysis process, degradation of ketamine was studied using visible, ultraviolet and sunlight irradiation by MoO₃ NPs as a nanophotocatalyst. It has been observed that degradation of ketamine was possible up to certain limiting value and it is enhanced through the presence of MoO₃ for the three irradiations. The maximum degradation is obtained for the optimal MoO₃ after 30 min of treatment due to the enhanced formation of hydroxyl radicals ($\cdot\text{OH}$), and hydroperoxyl radicals ($\cdot\text{O}_2\text{H}$) leading to an increase in the rates of

reactions with ketamine in the bulk solution or at the interface between the bubbles and the liquid phase [25,26]. It can be also established in the present work that under specific conditions i.e. with optimal catalyst, photocatalysis under sunlight has better efficacy as compared to the other irradiations with the catalyst (Fig. 5).

3.4. Analysis of Intermediates of Photocatalysis Process

In order to characterize the final and intermediates products of the photo degradation of ketamine, as well as to probe the degradation mechanism of the pharmaceutical product, a high-performance liquid chromatography (HPLC) was performed. Fig. 6 indicates the HPLC separations obtained for ketamine solution samples taken during photo degradation experiments. It can be observed that the main peak at the retention time $t_R = 7.49$ min, due to ketamine, decreases gradually and disappears after different light irradiation. There are several separation peaks appearing like (b) dehydronorketamine and (c) norketamine, which can be ascribed to the intermediates of the ketamine degradation (Fig. 6). As can be seen, degradation of ketamine under sunlight is fine and concentration of pathway is very low (Fig. 7). Therefore, this photocatalysis process is environmentally friendly.

3.5. Antibacterial Activity and Antifungal Studies

The antibacterial influence of synthesized MoO₃ NPs (10 μL) were quantitatively determined on the basis of the zone of inhibition (Table 1) which was compared control group. MoO₃ NPs exhibited strong antibacterial activity against both Gram positive and negative bacteria.

The antifungal activity of MoO₃ NPs was investigated against pathogenic *C.albicans* and *A. niger* by disc diffusion susceptibility method. The diameter of inhibition zones around each disc in the presence of MoO₃ NPs is determined. Table 1 shows the inhibition zone of control, MoO₃ NPs against on *C. albicans* and *A. niger*, respectively.

3.6. Antioxidant Activity

ABTS⁺ generated from the ABTS⁺ oxidation by potassium persulphate, is an excellent tool for distinguishing the antioxidant activity of chain breaking antioxidants and hydrogen-donating samples [27].

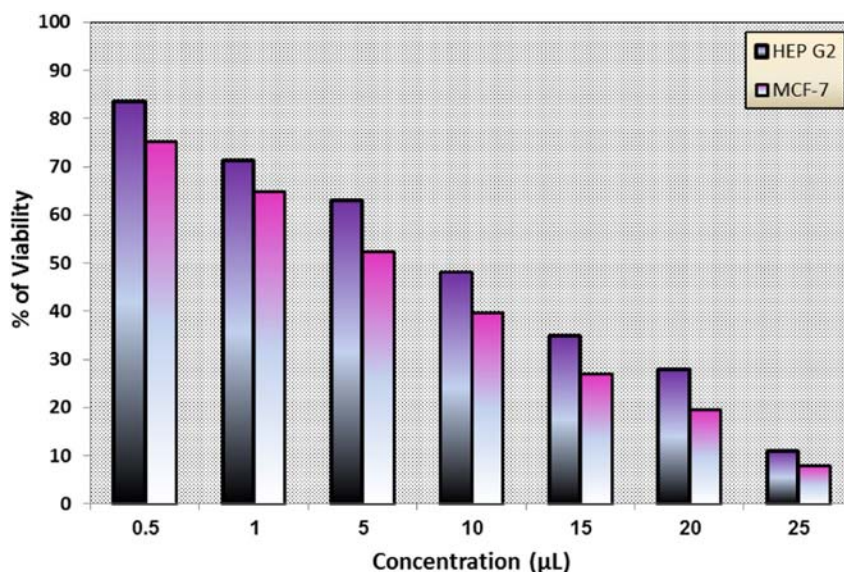


Fig. 9. Percentage of viability MoO₃ NPs on MCF-7 and HEP G2 cell line.

Free radical scavenging activity of the MoO₃ NPs on ABTS radicals was obtained to raise with increased in the concentration, demonstrating maximum inhibition (82.54%) at 1 mM and minimum inhibition (55.20%) at 0.125 mM solution (Fig. 8).

3.7. Cytotoxic Activity

The cytotoxicity activity of the MoO₃ nanoparticles on MCF-7 and HEP G2 cells were investigated by the MTT assay. The MCF-7 and HEP G2 cells showed reduction in viability of cells with increase in concentration of MoO₃ NPs. The percentage of viability at 25 µL was obtained to be 7.94 for MCF-7 and 10.88 for HEP G2 (Fig. 9). The result indicated that the root mediated prepared MoO₃ NPs possess best selectivity to cancer cell and can display potential property in chemotherapy and cancer chemoprevention.

4. Conclusions

The present research has shown that ketamine drug can be effectively degraded under source light irradiations (visible, UV and sunlight). It can be concluded that for effective degradation of ketamine, use of catalyst is vital. The particles were highly stable; then we feel MoO₃ NPs may be applied for the degradation of pharmaceutical effluents. The synthesized MoO₃ NPs exhibited excellent antimicrobial, anti-oxidant activity and also potent cytotoxicity against MCF-7 and HEP G2 finding its application as a potential chemo-preventive agent.

Acknowledgment

The authors gratefully acknowledge the support for this research by the Young Researchers and Elites club and Islamic Azad University, Science and Research Branch.

References

- [1] A. Fakhri, S. Behrouz, M. Pourmand, J. Photochem. Photobiol. B 149 (2015) 45.
- [2] A. Fakhri, M. Pourmand, R. Khakpour, S. Behrouz, J. Photochem. Photobiol. B 149 (2015) 78.
- [3] A.Y.C. Lin, X.H. Wang, C.F. Lin, Chemosphere 81 (2010) 562.
- [4] N. Perkas, G. Amirian, O. Girshevitz, J. Charmet, E. Laux, G. Guinert, H. Keppner, A. Gedanken, Surf. Coat. Technol. 205 (2011) 3190.
- [5] A.S. Nair, R. Jose, Y. Shengyuan, S. Ramakrishna, J. Colloid Interface Sci. 353 (2011) 39.
- [6] Q. Wang, Y.Z. Pan, S.S. Huang, S.T. Ren, P. Li, J.J. Li, Nanotechnology 22 (2011) 025501.
- [7] L. Xu, H. Song, B. Dong, Y. Wang, J. Chen, X. Bai, Inorg. Chem. 49 (2010) 10590.
- [8] T. Ressler, A. Walter, Z.-D. Huang, W. Bensch, J. Catal. 254 (2008) 170.
- [9] S.A. Toma's, M.A. Arvizu, O. Zelaya-Angel, P. Rodri'guez, Thin Solid Films 518 (2009) 1332.
- [10] J.X. Liu, Y. Ando, X.L. Dong, F. Shi, S. Yin, K. Adachi, T. Chonan, A. Tanaka, T. Sato, J. Solid State Chem. 183 (2010) 2456.
- [11] K. Sauvet, L. Sauques, A. Rougier, J. Phys. Chem. Solids 71 (2010) 696.
- [12] R.J. Elliot, Phys. Rev. 108 (1957) 1384.
- [13] C. Julien, A. Khelifa, O.M. Hussain, J.A. Nazri, J. Cryst. Growth 156 (1995) 235.
- [14] E. Reverchon, G. Della Porta, E. Torino, J. Supercrit. Fluoride 53 (2010) 95.
- [15] W.S. Kim, H.C. Kim, S.H. Hong, J. Nanoparticle Res. 12 (2010) 1889.
- [16] D. Parviz, M. Kazemeini, A.M. Rashidi, K.J. Jozani, J. Nanoparticle Res. 12 (2010) 1509.
- [17] A. Khademi, R. Azimirad, Y.T. Nien, A.Z. Moshfegh, J. Nanoparticle Res. 13 (2011) 115.
- [18] S. Li, C. Shao, Y. Liu, S. Tang, R. Mu, J. Phys. Chem. Solids 67 (2006) 1869.
- [19] M. Dhanasankar, K.K. Purushothaman, G. Muralidharan, Appl. Surf. Sci. 257 (2011) 2074.
- [20] M. Dhanasankar, K.K. Purushothaman, G. Muralidharan, Solid State Sci. 12 (2010) 246.
- [21] A. Fakhri, S. Behrouz, Sol. Energy 117 (2015) 187–191.
- [22] A. Fakhri, S. Behrouz, Sol. Energy 112 (2015) 163–168.
- [23] J.C. Manificier, M.D. Murcia, J.P. Fillard, E. Vicario, Thin Solid Films 41 (1997) 127–135.
- [24] A. Franco, M.C. Neves, M.M.L.R. Carrot, M.H. Mendonça, M.I. Pereira, O.C. Monteiro, J. Hazard. Mater. 161 (2009) 545–550.
- [25] M.A. Beckett, I. Hua, Environ. Sci. Technol. 34 (2000) 3944–3953.
- [26] N.H. Ince, G. Tezcanli-Guyer, R.K. Belen, I.G. Apikyan, Appl. Catal., B 29 (2001) 167–176.
- [27] L.P. Leong, G. Shui, Food Chem. 76 (2002) 75.